JOURNAL OF MATERIALS SCIENCE **40** (2005) 3783–3787

Structure and properties of EVOH/organoclay nanocomposites

HAN MO JEONG, BYEONG CHOON KIM, EUN HA KIM
Research Center for Machine Parts and Materials Processing, Department of Chemistry, University of Ulsan, Ulsan 680-749, Republic of Korea
E-mail: hmjeong@mail.ulsan.ac.kr

The nanocomposites of poly(ethylene-*co*-vinyl alcohol) (EVOH) with organoclay were prepared by a solution-precipitation method. The structures of nanocomposites were examined by X-ray diffraction. The exfoliation of organoclay was more evident in the nanocomposites of the EVOH containing 18 mol% vinyl alcohol (EVOH18), compared to the EVOH containing 5 mol% vinyl alcohol (EVOH5). Some of the bilayer alkylammonium structures at the clay gallery changed to monolayer structures in the nanocomposites. The thermal properties measured by differential scanning calorimetry showed the organoclay enhanced the crystallization of EVOH, however, it retarded crystallization when there was too much. The modulus of EVOH18 showed about a 2-fold increase of pristine polymer when using 7% of reinforcing organoclay.

1. Introduction

Nanocomposites based on organic polymers and layered silicates such as montmorillonite have attracted great interest. They exhibit improved performance properties compared to conventional composites because their unique phase morphology by layer intercalation or exfoliation maximizes interfacial contact between the organic and inorganic phases. As such, they greatly improve the thermal, mechanical, barrier as well as the flame-retardant properties of the polymers [1–9].

Since the polymer chains experience a significant loss of conformational entropy when the chains are intercalated into a narrow gallery between silicate layers, a large negative change of enthalpy is needed to overcome the entropy loss in order for the chains to diffuse into the gallery [10]. For most polar or polarizable polymers, organoclay is adequate to provide the sufficient excess enthalpy and to promote nanocomposite formation because organoclay is a layered silicate made to be organophilic by exchanging the interlayer cations with alkylammonium ions. However, it is not easy to disperse silicate layers homogeneously even with organoclay when the matrix polymer is comprised of nonpolar polyolefins. Because the silicate layers have hydroxy groups, the polymer needs to have a significant enough level of polar functionality that can interact with the silicate. As such, many studies have reported about the structure and properties of organoclay nanocomposites of polyolefins modified with polar functional groups such as maleic anhydride [11–15]. These are used as a compatibilizer in organoclay/nonpolar polyolefin nanocomposites.

Poly(ethylene-*co*-vinyl alcohol) (EVOH) has a hydroxy group that can interact with silicate layers. One study reported on the nanocomposite of EVOH that contained 68 mol% vinyl alcohol segment [16]. However, to the best of our knowledge, no paper has reported on the nanocomposite of EVOH whose major segment is ethylene. So, in this study, we prepared the nanocomposites of EVOH, whose vinyl alcohol content is 5 mol% or 18 mol% with varying amounts of organoclay. We observed the structure and the thermal and mechanical properties of the nanocomposites.

2. Experimental procedures

2.1. Materials

Poly(ethylene-*co*-vinyl alcohol) (EVOH) containing 18 mol% vinyl alcohol segment (EVOH18) was supplied by Polyscience Inc. Its intrinsic viscosity measured at 30 °C in phenol/1,1,2,2-tetrachloroethane (70/30 (v/v)) mixture was 98 cm^3/g [17]. EVOH containing 5 mol% vinyl alcohol segment (EVOH5) was obtained by the saponification of poly(ethylene-*co*-vinyl acetate) (Evaflex 550 of Mitsui). Its reduced viscosity measured at 70 °C with a solution of 4.0×10^3 g/cm^{-3} in toluene was 61 cm^3/g [18]. Organoclay, Cloisite 25A, was obtained from Southern Clay Products Inc. It was reported that in this organoclay the cations of natural montmorillonite were replaced by dimethyl, hydrogenated tallow, and 2-ethylhexyl quaternary ammonium ions. Its modifier concentration is 95 mmol/100 g-clay and its weight loss on ignition is 34%.

2.2. Preparation of nanocomposites

The nanocomposites were prepared by using a solution-precipitation method. The required amount of organoclay was dispersed in the 4% (w/v) toluene solution of EVOH at 100 °C. These solutions were added to

an excess (10-fold) of methanol, causing rapid coprecipitation. The precipitates were filtered, washed with methanol, and dried in a vacuum at 80 °C for 24 hrs.

2.3. Measurements

X-ray diffraction (XRD) patterns were obtained with an X-ray diffractomer (X'PERT, Philips) using Cu K_α radiation ($\lambda = 1.54$ Å) as the X-ray source. The diffraction angle was scanned from 1.2° at a rate of 1.2°/min.

Differential scanning calorimetry (DSC) was carried out with DSC-2100 (TA Instruments) at a heating and cooling rate of 10°C/min. Sample weights were 10.0 ± 0.5 mg. The glass transition temperature (T_g) was measured at the first heating scan to 150°C from −25°C. The temperature at the half-height of the heat capacity change was taken as the transition point. At the subsequent cooling scan down to −25°C, crystallization temperatures (T_c) and heat of crystallization (ΔH_c) were measured. The melting temperature (T_m) was measured at the next heating scan. In this second heating scan, T_g was not evident in the thermogram, probably due to high crystallinity. At least three samples for each specimen were scanned to confirm the reproducibility.

Tensile testing was done using a tensile tester (Instron 4411, Instron. Co., Ltd.). Micro-tensile specimens were prepared by the compression molding of precipitate at 130°C and had a rectangular shape with the dimensions of 30 mm length, 10 mm width, and 1.6 mm thickness. The specimen was elongated at the rate of 10 mm/min. For each data point, five samples were tested, and the average value was taken.

3. Results and discussion

3.1. XRD

The alkylammonium in the clay gallery can arrange differently depending on the charge density of clay and the structure of alkylammonium ions. Monolayer, bilayer, pseudo-trilayer, and paraffin structures can be illustrated as typical arrangements [19–21]. Simple calculations about the gallery heights using Bragg's law [Equation 1] suggest that $d_{\text{monolayer}} = 9.6 + 1 \times 4.6 = 14.2$ (Å) and the corresponding $2\theta = 6.2°$, and that $d_{\text{bilayer}} = 9.6 + 2 \times 4.6 = 18.8$ (Å) and the corresponding $2\theta = 4.7°$ [10, 22].

$$d = \frac{\lambda}{2 \sin \theta} \tag{1}$$

The organoclay used in this study, Cloisite 25A, has a peak of around $2\theta = 4.7°$ in the XRD pattern shown in Fig. 1a, which suggests that alkylammonium ions have a bilayer arrangement. When some amounts of EVOH18 are blended, in Fig. 1b, the intensity at low angles of XRD patterns is increased. In Fig. 1c this intensity increases at a low angle is more evident and the peak position moves slightly to a lower angle. These show that the gallery gap is expanded by intercalated EVOH18 molecules. Fig. 1d shows that EVOH18/organoclay nanocomposite has two peaks located around 3.1° and 5.2° in the XRD pattern when

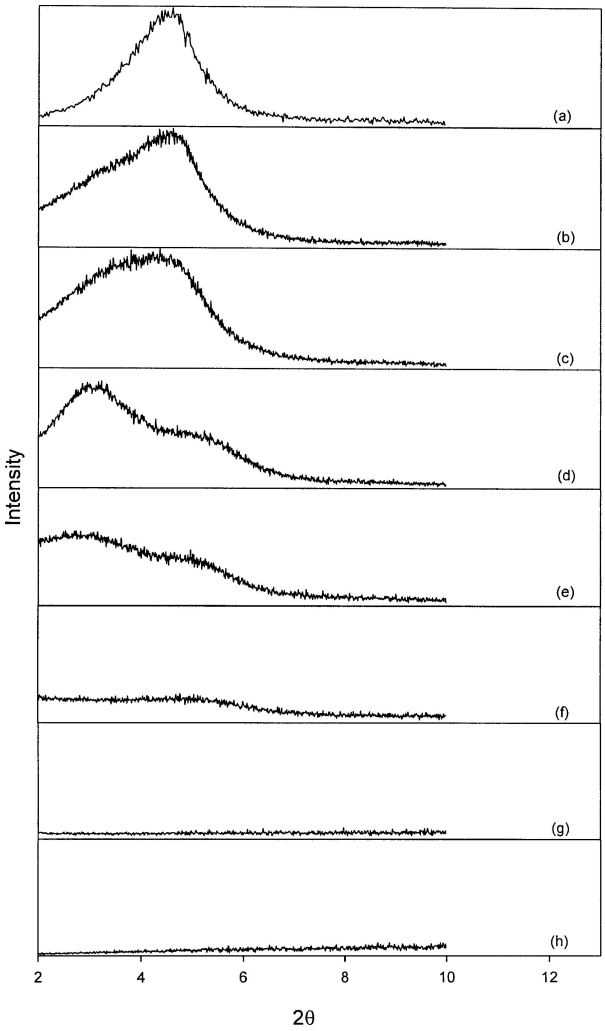

Figure 1 XRD patterns of EVOH18/organoclay nanocomposites: (a) 0/100, (b) 5/95, (c) 10/90, (d) 30/70, (e) 70/30, (f) 90/10, (g) 95/5, (h) 100/0 by weight.

the composition of EVOH18/organoclay is 30/70 by weight. The peak at around 3.1° shows that the gallery gap is more expanded at this composition by the intercalated EVOH18. However the peak at around 5.2° cannot be considered as the 002 reflection of the intercalated structure because the peak does not correspond to the scattering angle two times that of the first peak [10]. The peak at around 5.2° suggests that some of the bilayer arrangement changes to a monolayer arrangement. This peak of around 5.2° seems to be due to the intercalated structure of the monolayer arrangement [10, 22, 23]. In Fig. 1e, a relative peak intensity below 3°, compared to an intensity of above 3°, is increased when compared to Fig. 1d. This shows that the amount of exfoliated structure is increased in a 70/30 blend compared to a 30/70 blend. When the composition is 90/10, in Fig. 1f, peak of around 3.1° disappear and peak of around 5.2° are much reduced. This shows that much of the organoclay is exfoliated, however some of the intercalated monolayer structures remained. In Fig. 1g, no evident peak was observed in the XRD pattern. This shows that almost all the organoclay has been exfoliated when the composition of EVOH18/organoclay is 95/5 by weight.

Fig. 2 shows the XRD patterns of EVOH5/organoclay nanocomposites. We can see in Fig. 2b that the

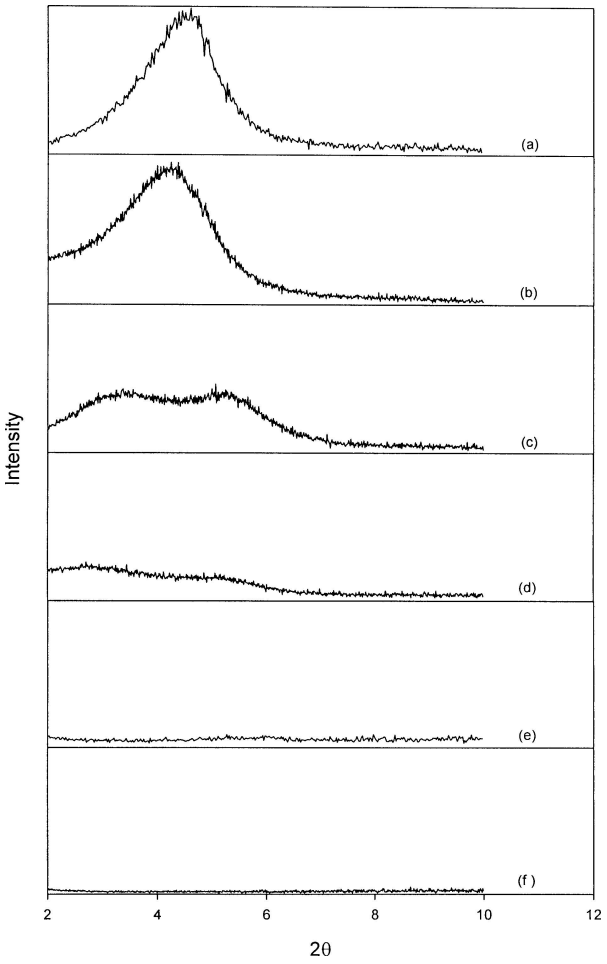

Figure 2 XRD patterns of EVOH5/organoclay nanocomposites: (a) 0/100, (b) 10/90, (c) 70/30, (d) 95/5, (e) 99/1, (f) 100/0 by weight.

peak position moves to a lower angle by the development of an intercalated structure of bilayer arrangement. When the composition of EVOH/organoclay is 70/30 by weight, two peak were observed due to the intercalated structure of bilayer and monolayer arrangements, in Fig. 2c, at angles around 3.4° and 5.2°, respectively. In Fig. 2d, two peaks at angles around 2.8° and 5.1° were also observed when the composition of EVOH18/organoclay is 95/5. Fig. 2e also showed a small peak around 5.6°. This shows that an exfoliated structure does not develop fully even at these compositions. When the results of Fig. 2 are compared to those of Fig. 1, we can see that the development of an intercalated or exfoliated structure is relatively difficult for EVOH5 compared to EVOH18 because of the low content of a hydroxy group. In the previous report on EVOH/organoclay nanocomposite [16], intercalated rather than exfoliated structures were mostly observed, even when the content of vinyl alcohol in EVOH was 68 mol%.

3.2. Thermal properties

Fig. 3 shows the DSC thermograms of EVOH/organoclay nanocomposites and the thermal properties measured are summarized in Table I. The super-cooling necessary for crystallization, $T_m - T_c$, decreases when the content of organoclay increases up to around 10%. This suggests that a silicate layer of organoclay acts

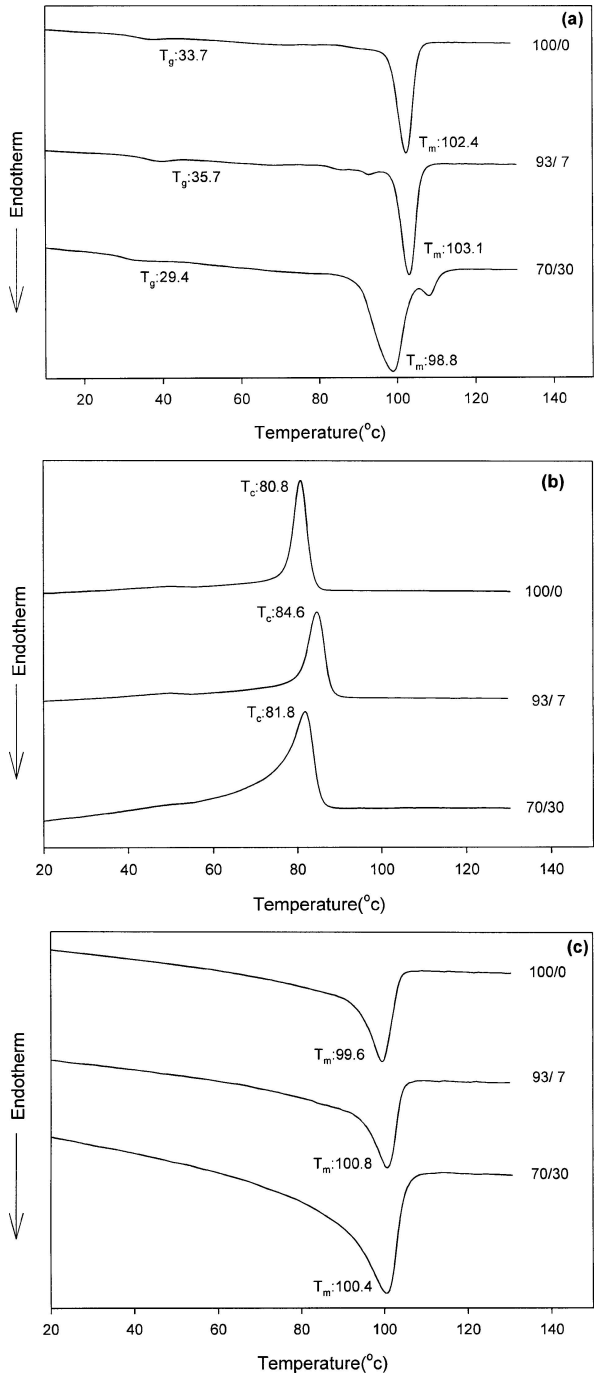

Figure 3 DSC thermograms of EVOH18/organoclay nanocomposite (100/0, 93/7, 70/30 by weight): (a) first heating scan, (b) cooling scan, (c) second heating scan.

as a nucleating agent for the heterogeneous nucleation [24–27]. However, the super-cooling increases again when the organoclay clay content increases more than about 10%. This suggests that organoclay hinders the diffusion and the rearrangement of polymer chains for crystallization, when there is too much of it. As the content of organoclay is increased, Table I, the heat of crystallization, ΔH_c, decreases after the first increase. This variation of ΔH_c also shows that small amounts of organoclay enhances the crystallization of EVOH, however, too much organoclay hinders crystallization. This adverse effects of organoclay on the crystallization of EVOH were more evidently observed in the previous report [16], where the content of vinyl alcohol in the EVOH was 68 mol%. This may be due to the

TABLE I Thermal properties of EVOH/organoclay nanocomposites

Composition by weight	T_g (°C)	T_c (°C)	T_m (°C)	$T_m - T_c$ (°C)	ΔH_c (J/g-EVOH)
EVOH18/organoclay					
100/0	33.7	80.8	99.6	18.8	56.3
99/1	35.5	80.5	99.3	18.8	57.3
97/3	35.3	82.6	100.5	17.9	58.1
95/5	35.4	84.5	100.7	16.2	59.3
93/7	35.7	84.6	100.8	16.2	60.0
85/15	30.4	83.8	100.4	16.1	57.8
80/20	28.3	82.8	100.3	17.5	51.0
70/30	29.4	81.8	100.4	18.6	48.2
50/50	29.9	78.5	97.2	18.7	46.8
30/70	31.6	72.7	91.6	18.9	29.9
10/90	37.0	–	–	–	0.0
EVOH5/organoclay					
100/0	–	94.0	106.9	12.9	100.0
99/1	–	94.8	107.0	12.2	101.0
97/3	–	95.7	107.2	11.5	101.8
95/5	–	95.8	107.1	11.3	104.2
93/7	–	95.6	107.3	11.7	104.9
85/15	–	93.9	106.8	12.9	112.3
80/20	–	93.9	106.8	12.9	108.5
70/30	–	93.7	106.8	13.1	102.7
50/50	–	91.9	105.2	13.3	101.9
30/70	–	90.8	104.2	13.4	101.8
10/90	–	79.0	99.4	20.4	64.9
5/95	–	72.2	94.2	22.0	59.8

TABLE II Tensile properties of EVOH18/organoclay nanocomposites

Composition by weight	Modulus (GPa)	Elongation at break (%)
100/0	0.74	317
99/1	0.93	341
97/3	0.98	320
95/5	1.05	217
93/7	1.35	189

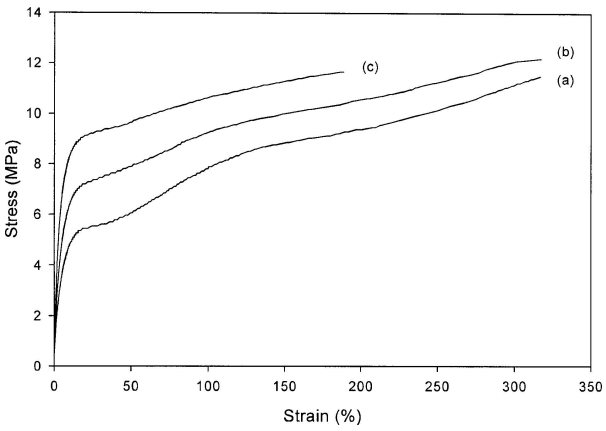

Figure 4 Stress-strain curves of EVOH18/organoclay nanocomposites: (a) 100/0, (b) 97/3, (c) 93/7 by weight.

stronger interactions between organoclay and EVOH with higher content of polar vinyl alcohol repeating unit. The melting temperature also similarly varies as the content of organoclay is increased (Table I). That is, it decreases after the first increase as in the variation of ΔH_c. The Gibbs free energy of melting ΔG_m is given by

$$\Delta G_m = \Delta H_m - T_m \Delta S_m \tag{2}$$

where ΔH_m, ΔS_m are enthalpy and entropy changes accompanied by melting. At the melting temperature, $\Delta G_m = 0$: so

$$T_m = \frac{\Delta H_m}{\Delta S_m} \tag{3}$$

When chain mobility is restricted by organoclay, it can be anticipated that ΔS_m will be decreased compared to the pristine polymer. So, a decrease of ΔS_m by restricted chain mobility in the presence of organoclay may be suggested as a cause of a T_m increase when a small amount of organoclay is added. We observed that the crystallite size decreases as the content of organoclay is increased in polyurethane/organoclay nanocomposites. Because T_m decreases as the crystallite size is decreased [28], a decrease of T_m at high content levels of organoclay may be assumed to be due to the reduced crystallite size of EVOH in the presence of organoclay. Further experiments, however, will be necessary to support this assumption. In Table I we have noted that the glass transition temperature, T_g, of EVOH18/organoclay nanocomposites increases as the content of organoclay is increased up to 7%. It decreases at intermediate composition and increases again at a high content of organoclay. Because T_g can be increased by the restricted mobility of EVOH18 molecules in the presence of organoclay [29, 30] and by an increased crystallinity, these two may be suggested as causes of T_g increases when a small amount of organoclay is added. Decreased crystallinity may be suggested as a cause of T_g decreases at the intermediate content of organoclay. Previous report on EVOH/organoclay nanocomposite explained the plasticizing effect of the low molecular weight organic cations as a cause of T_g decrease [16]. A second increase of T_g seems to be due to the predominant effects of the restricted chain mobility of EVOH18 at a high content of organoclay.

3.3. Tensile properties

The stress-strain curves of EVOH18/organoclay nanocomposites are shown in Fig. 4 and the tensile properties measured are shown in Table II. The tensile modulus increases about 2-fold of the pristine polymer when the content of organoclay is increased up to 7% [6, 11]. However, the elongation at break decreases after the first increase. This is probably due to the restricted chain mobility in the presence of organoclay.

4. Conclusion

In the EVOH/organoclay nanocomposites made by a solution-precipitation method, we observed that:

1. Some of the bilayer structure of alkylammonium ions in the clay gallery changed to a monolayer structure.

2. The crystallization of EVOH was enhanced by small amounts of organoclay, however, organoclay retarded crystallization when there was too much of it.

3. About a 2-fold modulus increase of EVOH18 was attained with 7% organoclay.

Acknowledgements

This work was supported by the Korea Science and Engineering Foundation (KOSEF) through the Research Center for Machine Parts and Materials Processing (ReMM) at the University of Ulsan.

References

1. E. P. GIANNELIS, *Appl. Organometal. Chem.* **12** (1998) 675.
2. Y. KOJIMA, A. USUKI, M. KAWASUMI, A. OKADA, T. KURAUCHI and O. KAMIGAITO, *J. Polym. Sci., Polym. Chem.* **31** (1993) 983.
3. T. LAN and J. PINNAVAIA, *Chem. Mater.* **6** (1994) 2216.
4. H. ISHIDA, S. CAMPBELL and J. BLACKWELL, *ibid.* **12** (2000) 1260.
5. H. R. DENNIS, D. L. HUNTER, D. CHANG, S. KIM, J. L. WHITE, J. W. CHO and D. R. PAUL, *Polymer* **42** (2001) 9513.
6. B. K. KIM, J. W. SEO and H. M. JEONG, *Eur. Polym. J.* **39** (2003) 85.
7. J. W. GILMAN, C. L. JACKSON, A. B. MORGAN, R. HARRIS, JR., E. MANIAS, E. P. GIANNELIS, M. WUTHENOW, D. HILTON and S. H. PHILLIPS, *Chem. Mater.* **12** (2000) 1866.
8. J. G RYU, J. W. LEE and H. KIM, *Macromol. Res.* **10** (2002) 187.
9. S.-C. CHUNG, W.-G. HAHM S.-S. IM and S.-G. OH, *ibid.* **10** (2002) 221.
10. J. T. YOON, W. H. JO, M. S. LEE and M. B. KO, *Polymer* **42** (2001) 329.
11. E. MANIAS, A. TOUNY, L. WU, K. STRAWHECKER, B. LU and T. C. CHUNG, *Chem. Mater.* **13** (2001) 3516.
12. M. KAWASUMI, N. HASEGAWA, M. KATO, A. USUKI and A. OKADA, *Macromolecules* **30** (1997) 6333.
13. D. MARCHANT and K. JAYARAMAN, *Ind. Eng. Chem. Res.* **41** (2002) 6402.
14. K. H. WANG, M. H. CHOI, C. M. KOO, Y. S. CHOI and I. J. CHUNG, *Polymer* **42** (2001) 9819.
15. P. REICHERT, B. HOFFMANN, T. BOCK, R. THOMANN, R. MÜLHAUPT and C. FRIEDRICH, *Macromol. Rapid Commun.* **22** (2001) 519.
16. N. ARTZI, Y. NIR, M. NARKIS and A. SIEGMANN, *J. Polym. Sci., Polym. Phys.* **40** (2002) 1741.
17. S.-B. AHN and H. M. JEONG, *Korea Polym. J.* **6** (1998) 389.
18. T. O. AHN and H. M. JEONG, *Polymer* (Korea) **11** (1987) 112.
19. P. C. LEBARON, Z. WANG and T. P. PINNAVAIA, *Appl. Clay* **15** (1999) 11.
20. R. A. VAIA, R. K. TEUKOLSKY and E. P. GIANNELIS, *Chem. Mater.* **6** (1994) 1017.
21. G. LAGALY, *Solid State Ionics* **22** (1986) 43.
22. M. B. KO, M. PARK, J. KIM and C. R. CHOE, *Kor. Polym. J.* **8** (2000) 95.
23. K. N. KIM, H. KIM and J.-W. LEE, *Polym. Eng. Sci.* **41** (2001) 1963.
24. J. LI, C. ZHOU and W. GANG, *Polym. Test.* **22** (2003) 217.
25. J. MA, S. ZHANG, Z. QI, G. LI and Y. HU, *J. Appl. Polym. Sci.* **83** (2002) 1978.
26. W. XU, M. GE and P. HE, *J. Polym. Sci., Polym. Phys.* **40** (2002) 408.
27. P. MAITI, P. H. NAM, M. OKAMOTO, N. HASEGAWA and A. USUKI, *Macromolecules* **35** (2002) 2042.
28. B. WUNDERLICH "Macromolecular Physics, Crystal Melting" (Academic Press, Inc., New York, 1980) Vol 3.
29. X. HUANG and W. J. BRITTAIN, *Macromolecules* **34** (2001) 3255.
30. M. W. NOH and D. C. LEE, *Polym. Bull.* **42** (1999) 619.

Received 14 July 2003
and accepted 3 February 2005